Adsorption of Associating Fluids on Solid Surfaces: Wetting Transition from Density Functional Theory

Andrzej Patrykiejew and Stefan Sokołowski*

Department for the Modelling of Physico-Chemical Processes, Maria Curie-Skłodowska University, 20031 Lublin, Poland

Received: May 27, 1998; In Final Form: March 11, 1999

Adsorption of associating hard spheres and particles interacting via the Lennard-Jones potential at a Lennard-Jones adsorbing wall is studied using the density functional theory. A model of association with one site per particle is considered. To test the theory we have also performed Monte Carlo simulation in the canonical ensemble for a Lennard-Jones associating fluid at high temperatures and for hard associating spheres. Next, the influence of association on the wetting behavior of the fluid−solid interface is investigated. It is shown that the prewetting transition in associating systems is considerably influenced by the association processes.

1. Introduction

The structure of associating fluids near adsorbing surfaces has been intensively studied by computer simulations as well as by various theories of inhomogeneous fluids. Theoretical approaches have been most often based on the application of singlet or pair integral equations for the density profile (see, for example, refs 1−5). Recently, this problem has been also attacked using one of the most powerful and popular theoretical approaches, so widely used in the case of simple and nonuniform fluids, namely the density functional (DF) theory.[6−13]

The first DF-type approach for nonuniform associating fluids has been proposed by Kierlik and Rosinberg[7−9] who applied the DF theory to describe an inhomogeneous fluid of fully associated nonoverlapping hard spheres. Although that theory self-consistently determines density profiles at a hard wall, the obtained contact densities disagree with bulk pressures unless adjustable parameters are used. More recently, Segura, Chapman, and co-workers[11,12] have presented a new and successful version of the DF theory describing the adsorption of associating fluids. The performed tests of that theory have shown that in the case of associating hard spheres near a hard wall a generally good agreement between theoretical predictions and Monte Carlo data are obtained.

In the case of simple fluids, the wetting behavior of model fluid−solid interfaces has been debated a great deal in the literature on inhomogeneous fluids—for a review see, e.g., ref 6. Several systems, including energetically and geometrically heterogeneous surfaces and colloidal particles have been studied.[14−20] The investigations have been carried out by using theoretical approaches, mainly based on different versions of the DF theory, as well as on computer simulation techniques.[20−26] One of the problems the discussion has focused on was the state conditions of an adsorbate, at which the adsorbed film undergoes a surface wetting transition. According to the recent theories, the order of wetting transition depends upon the relative strengths and ranges of the interparticle and the wall−particle forces.[6,20] In the case of the first-order wetting transition the prewetting line is usually located close to the bulk gas−liquid coexistence line.

In this work, we study a simple model of the Lennard-Jones (LJ) associating fluid, with angular-dependent associative forces, being in contact with the Lennard-Jones adsorbing surface. We focus the attention on the investigation of the influence of the chemical association (dimerization) on the wettability of a structureless wall. We calculate the density profiles and adsorption isotherms and evaluate the phase diagrams. This is done by using the density functional theory outlined in refs 11−13. Moreover, to test the proposed theoretical approach we perform comparisons of the theoretical predictions for associating hard spheres and LJ particles at temperatures well above the bulk critical temperature with the results of canonical ensemble Monte Carlo simulation. To our best knowledge the studies presented here comprise the first in the literature trial to investigate the influence of association on the wettability of adsorbing surfaces via the density functional method.

2. Theory

2.1. The Model. We consider the system of particles interacting via the following pair potential

$$u(\mathbf{r},\boldsymbol{\omega}_1,\boldsymbol{\omega}_2) = u_{\text{non}}(r) + \sum_{\text{A}}\sum_{\text{A}'} u_{\text{AA}'}(\mathbf{r},\boldsymbol{\omega}_1,\boldsymbol{\omega}_2) \qquad (1)$$

where r is the magnitude of the vector $\mathbf{r}$ connecting the centers of molecules 1 and 2 and $\boldsymbol{\omega}_i$, $i = 1, 2$, are the orientations of molecules 1 and 2 relative to the vector $\mathbf{r}$. The double sum runs over all association sites belonging to each molecule, u_{non} is the nonassociative part of the potential. The majority of the calculations presented below have been carried out assuming that $u_{\text{non}}(r)$ is just a truncated LJ (12,6) potential

$$u_{\text{non}}(r) = u_{\text{LJ}}(r) = \begin{cases} 4\epsilon[(\sigma/r)^{12} - (\sigma/r)^6] & r < r_{\text{cut}} \\ 0 & r > r_{\text{cut}} \end{cases} \qquad (2)$$

where the cutoff distance is assumed to be $r_{\text{cut}} = 2.5\sigma$. Some of the test calculations have been carried out for associating hard spheres, i.e., for the potential

$$u_{\text{non}}(r) = u_{\text{HS}}(r) = \begin{cases} \infty & r < \sigma \\ 0 & r > \sigma \end{cases} \qquad (3)$$

* Corresponding author. E-mail: stefan@paco.umcs.lublin.pl.

10.1021/jp982382p CCC: $18.00
Published on Web 05/04/1999

Without loss of generality we assume that in both cases σ is the unit of length, i.e., $\sigma = 1$.

One associative site per particle is considered and the associative potential is given by[11−13,27−31]

$$u_{as}(\mathbf{12}) = u_{as}(x_{12}) = \begin{cases} -\epsilon_a & x_{12} \le a \\ 0 & x_{12} > a \end{cases} \tag{4}$$

Here $x_{12} = |\mathbf{r}_{12} + \mathbf{d}(\omega_1) - \mathbf{d}(\omega_2)|$, $\mathbf{d}(\omega)$ denotes the position and orientation of the attractive interaction site, ϵ_a and a are the association energy and the range of attraction, respectively, and the distance between the center of the molecule and the associative site is L. In this work, we choose the following set of parameters: $L = 0.5$ and $a = 0.1$. These parameters ensure steric saturation at the dimer level.[27]

The fluid is adsorbed by a structureless surface, which is the source of the Lennard-Jones (9,3) potential field

$$v(z_i) = \frac{3^{3/2}}{2}\epsilon_s\left[\left(\frac{z_0}{z_i}\right)^9 - \left(\frac{z_0}{z_i}\right)^3\right] \tag{5}$$

where z_i is the distance of the particle i from the surface. In this work we assume that $z_0 = 0.8$ and that $(3\sqrt{3}/2)\epsilon_s/k = 6$, where k is the Boltzmann constant.

2.2. Density Functional Theory. The most commonly used methods proposed for approximating the free energy for the simple classical inhomogeneous systems can be classified into three groups. In the first group[32] the free energy for the inhomogeneous system is written as a perturbation to the free energy about a given uniform reference homogeneous system. In the second group of approximations[15,33−37] the free energy functional is written as a function of an effective or weighted density, which is itself an averaged functional of the local density. Different averaging methods have been proposed, all of these make use of some properties of a reference homogeneous state and a specific assumed averaged density function. The third group of approximations[17,38,39] is based upon the functional expansion of the chemical potential around a local reference density. The weighting function and the weighted density are determined by the external condition of the free energy with respect to the "coarse-grained" density. In this group of approximations the knowledge of a reference homogeneous state as input is assumed. Apart from the approaches quoted above, there exist methods starting from some other basic principles, for example, theory due to Rosenfeld, Kierlik, and Rosinberg, which makes use of geometric considerations.[40−43]

In the majority of the density functional approaches based on the weighted density, a perturbation treatment of the interparticle forces has been employed. The interparticle potential has been divided into repulsive and attractive terms. For simplicity, the attractive potential, $u_{att}(r)$ has been hitherto treated mostly in a mean-field approximation, which assumes the pair correlation function for this part of the potential to be unity everywhere. This assumption leads to a model system in which hard spheres are moving in a nonuniform background potential, created by the external potential as well as by the mean-field potential. Several trials to improve the mean-filed approximations have been also undertaken.[44−47]

There has also been discussed a possibility of construction of a density functional theory with weighted density approximation that does not require application of the perturbational treatment. Indeed, Curtin and Ashcroft[33] presented their theory in terms of the full free energy functional rather than the hard-sphere part. However, it is clear that making use of the density functional approach on the full functional would require some prescription for the two-particle direct correlation function and the uniform system free energy for densities corresponding to two-phase states of the bulk phase diagram. The division of the interparticle potential into hard-sphere and attractive portions avoids the above mentioned difficulties and is essential for accurate structure of the adsorbed layer. In a latter paper Curtin and Ashcroft[44] calculated the bulk freezing properties and the liquid−gas coexistence curve for a Lennard-Jones fluid, applying a perturbation treatment with a hard-sphere reference fluid. Perturbational treatment is also used in the present theory.[11,12] Similarly, as in the case of the theory of bulk associating fluids,[27−30] we treat both attractive van der Waals forces and associative potential as perturbation and expand the free energy of an associating fluid around that of hard spheres. More precisely, this theory combines the density functional approach developed by Evans and Tarazona[6,15,16] with the Wertheim[27−30] theory of association. Because both the above mentioned approaches are now quite standard, we present only basic points of the theory.

To begin, we start from the definition of the grand potential Ω as a functional of the number density of a fluid $\rho(\mathbf{r})$.[6]

$$\Omega = F + \int \rho(\mathbf{r})[v(z) - \mu]\, d\mathbf{r} \tag{6}$$

where μ is the chemical potential. The Helmholtz free energy, F, is broken up into a sum of ideal and excess parts: $F = F^{id} + F^{ex}$, where

$$F^{id}/kT = \int \rho(\mathbf{r})[\log \rho(\mathbf{r}) - 1]\, d\mathbf{r} \tag{7}$$

The excess free energy is divided into parts representing the contributions due to repulsive, attractive nonassociative forces acting between molecules, as well as into the contribution arising from the association,[11−13] $F^{ex} = F^{ex}_{rep} + F^{ex}_{att} + F^{ex}_{ass}$. The first step toward the development of appropriate expressions is the division of the nonassociative pair potential into repulsive and attractive terms. In this work we apply the Weeks−Chandler−Andersen (WCA) division,[48] according to which the attractive part of the potential is defined by

$$u_{att}(r) = \begin{cases} -\epsilon & r < r_{min} \\ u_{LJ}(r) & r > r_{min} \end{cases} \tag{8}$$

where $r_{min} = 2^{1/6}\sigma$.

The repulsive forces, $u_{rep}(r) = u_{LJ}(r) - u_{att}(r)$, are usually[6] modeled by a hard-sphere potential. The contribution F^{ex}_{rep} is computed in a nonlocal manner by employing the concept of smoothed density,[6,11−13,15,49] $\tilde{\rho}(\mathbf{r})$, i.e., the density obtained by averaging the local density with a weight function w,

$$\tilde{\rho}(\mathbf{r}) = \int d\mathbf{r}'\, \rho(\mathbf{r}')\, w[|\mathbf{r} - \mathbf{r}'|, \tilde{\rho}(\mathbf{r})] \tag{9}$$

According to Tarazona et al.,[15,49] the weight function w is expanded into the following power series[15,49]

$$w(r, \tilde{\rho}) = w_0(r) + w_1(r)\tilde{\rho} + w_2(r)\tilde{\rho}^2 \tag{10}$$

where the coefficients w_0, w_1, and w_2 are evaluated so as to ensure a good description of the direct correlation function of a bulk hard sphere fluid. The numerical values of these coefficients can be found in ref 49.

The equation defining F^{ex}_{rep} takes the form:

$$F^{ex}_{rep} = \int d\mathbf{r}\, \rho(\mathbf{r})\, f^{ex}_{rep}[\tilde{\rho}(\mathbf{r})] \tag{11}$$

where f^{ex}_{rep} is the free energy density of hard spheres of diameter d and is evaluated from the Carnahan−Starling equation:[50]

$$f^{ex}_{rep}(\rho)/kT = \eta(4 - 3\eta)/(1 - \eta)^2 \tag{12}$$

where $\eta = \pi\rho/4$. In principle, the effective hard-sphere diameter can be optimized,[6] but in this work we simply set it as equal to σ.

The nonassociative attractive forces are treated in a mean-field fashion,[6] i.e.

$$F^{ex}_{att} = \int d\mathbf{r}\, f^{ex}_{att}(\mathbf{r}) \tag{13}$$

where

$$f^{ex}_{att} = \frac{1}{2}\int d\mathbf{r}'\, \rho(\mathbf{r})\, \rho(\mathbf{r}')\, u_{att}(|\mathbf{r} - \mathbf{r}'|) \tag{14}$$

Finally, the associative term is given by[11−13]

$$F^{ex}_{ass} = \int d\mathbf{r}\, \rho(\mathbf{r})\, f^{ex}_{ass}[\tilde{\rho}(\mathbf{r})] \tag{15}$$

where

$$f^{ex}_{ass}(\tilde{\rho})/kT = [\ln \chi(\tilde{\rho}) - \chi(\tilde{\rho})/2 + 0.5] \tag{16}$$

Equation 15 means that the associative free energy contribution is computed using the weighted density obtained via the hard-sphere weighted function (10). One could consider a possibility of application of a different averaged density to evaluate this free energy contribution. In this work, however, we follow the theory outlined in refs 11−13: do not consider the option mentioned above. The variable χ in the above is the fraction of molecules not bonded at the associative site. According to refs 11−13 $\chi(\tilde{\rho})$ is obtained from an equation quite analogous to that in the case of bulk associating fluids,[28,29] i.e., from

$$\chi(\tilde{\rho}) = \frac{1}{1 + \tilde{\rho}\chi\Delta(\tilde{\rho})} \tag{17}$$

where $\Delta(\tilde{\rho})$ is approximated by

$$\Delta(\tilde{\rho}) \approx [\exp(-\epsilon_a/kT) - 1]\left(\frac{\pi}{6L^2}\right)\int_{2L-a}^{2L+a} g(r;\tilde{\rho}) \times (a + 2L - r)^2(2a - 2L + r)r\, dr \tag{18}$$

with g being the pair distribution function of the system interacting via the potential $u_{rep}(r)$ at the density $\tilde{\rho}$. This function is assumed to be given by[28,29]

$$g(r) \approx \exp[-u_{rep}(r)/kT]y_d(r) \tag{19}$$

with $y_d(r)$ being the Percus−Yevick hard-sphere cavity function at the density $\tilde{\rho}$. Although the Percus−Yevick cavity function is not accurate for hard spheres, but Chapman[51] showed that when used to approximate $g(r)$, it produces more accurate results than the cavity function from computer simulations.

The equilibrium density profile is obtained by minimizing the grand potential, $\delta\Omega/\delta\rho(z) = 0$, and hence we obtain

$$-kT\ln[\rho(z)/\rho_b] = v(z) + f^{ex}[\tilde{\rho}(z)] - f^{ex}(\rho_b) + \int d\mathbf{r}'\, u_{att}(\mathbf{r}' - \mathbf{r}|)[\rho(z) - \rho_b] + \int \frac{\delta\tilde{\rho}(z')}{\delta\rho(z)}(f^{ex}_{rep}[\tilde{\rho}(z')] + f^{ex}_{ass}[\tilde{\rho}(z')])'\, \rho(z')\, dz' - \rho_b[f^{ex}_{rep}{}'(\rho_b) + f^{ex}_{ass}{}'(\rho_b)] \tag{20}$$

where $f^{ex\prime}$ is the excess free energy derivative with respect to the density and ρ_b is the bulk (reference) density, corresponding to the chemical potential μ.

One of the main ingredients of the theory quoted above is the Tarazona weighted density functional method. In fact, Tarazona's theory is one of many successful approaches and the hard-sphere contribution to the free energy of an associating fluid can be estimated by using other well-known theories (cf. ref 6), as the modified Meister−Kroll theory, for example.[13] However, among different approaches, the Tarazona theory is one of the simplest and the most accurate ones. Moreover, the results of calculations presented in refs 11−13 for hard associating spheres near a hard wall have indicated that the above described theory works reasonably good. Discrepancies between the theory and simulations have occurred at high association energies and low bulk fluid densities ρ_b, where a crossover from desorption to adsorption takes place. However, it should be checked if this theory will be successful also in the case of associating hard spheres near LJ adsorbing surface, as well as in the case of LJ associating fluid adsorbed on attractive walls. Of course, the phase behavior of a LJ nonuniform fluid predicted by the DF theory must substantially differ from the results of computer simulations.[6] Nevertheless, we can expect that the qualitative picture emerging from the DF calculations should be correct. Therefore, the below presented results of DF theory are compared with computer simulation only for hard sphere systems and for the LJ system above the critical temperature.

3. Results and Discussion

3.1. Computer Simulation vs DF Theory. We have performed computer simulations for hard associating spheres, as well as for LJ associating fluids. The realization of Monte Carlo displacement step used in this paper is identical with that described in refs 31, 52, and 53.

The simulated system consists of a rectangular box with the long (z) axis bounded by the walls (external fields) and with periodic boundary conditions in the x and y directions. The bottom wall of the box is the adsorbing surface. The system is closed from the top by a hard, reflecting wall. The box size, $xl = yl = 10\sigma$, $zl = 20\sigma$, the number of the particles N, and the temperature T are specified at the beginning of the calculation. An initial configuration of N particles is also chosen, as well as the particle translation parameter. The last parameter has been selected to assure the total acceptance ratio at the level of 25−30%. At least 4×10^5 Monte Carlo steps, each of which has consisted of N trials to move a particle have been carried out to obtain final averages. During each run we have evaluated the density profiles of all particles as well as those for undimerized species.

The first series of our calculations has been carried out for associating hard spheres. Figure 1 shows a comparison of the simulated and theoretical density profiles of all (free and associated) particles and the profiles of associated species, $(1 - \chi(z))\rho(z)$, for two selected systems. The bulk equilibrium densities of associated particles predicted by theory agree well with simulations. This agreement confirms that the bulk theory

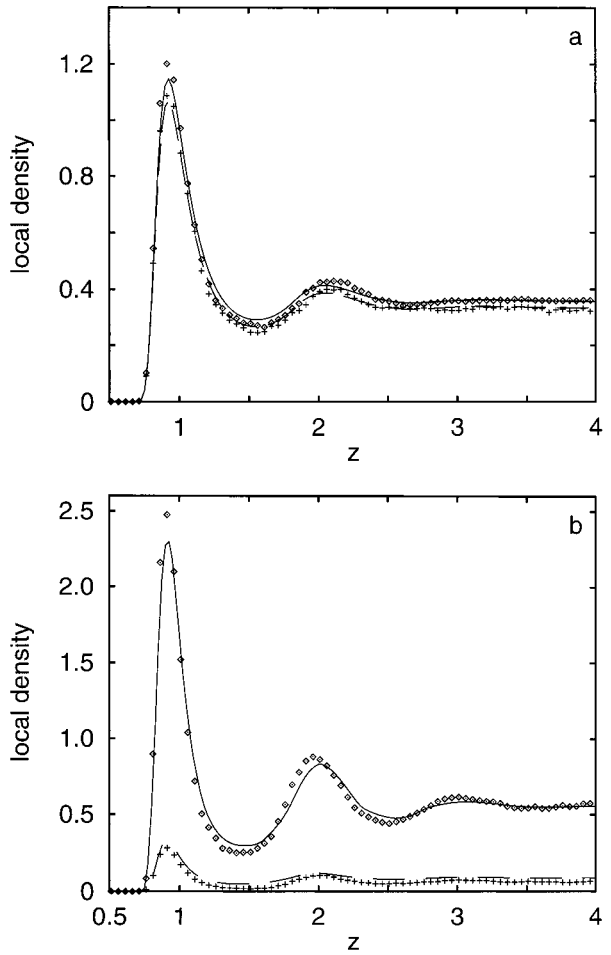

Figure 1. A comparison of the density profiles of all particles (solid lines and diamonds) and monomer density profiles (dashed lines and crosses) of associating hard spheres resulting from theory (lines) and from Monte Carlo simulations (points). The calculations have been carried out for $\epsilon_s/kT = 4$, $\epsilon_a/kT = 10/1.5$, and $\rho_b^* = 0.355$ (part a) and for $\epsilon_s/kT = 6$, $\epsilon_a/kT = 12$, and $\rho_b^* = 0.565$ (part b).

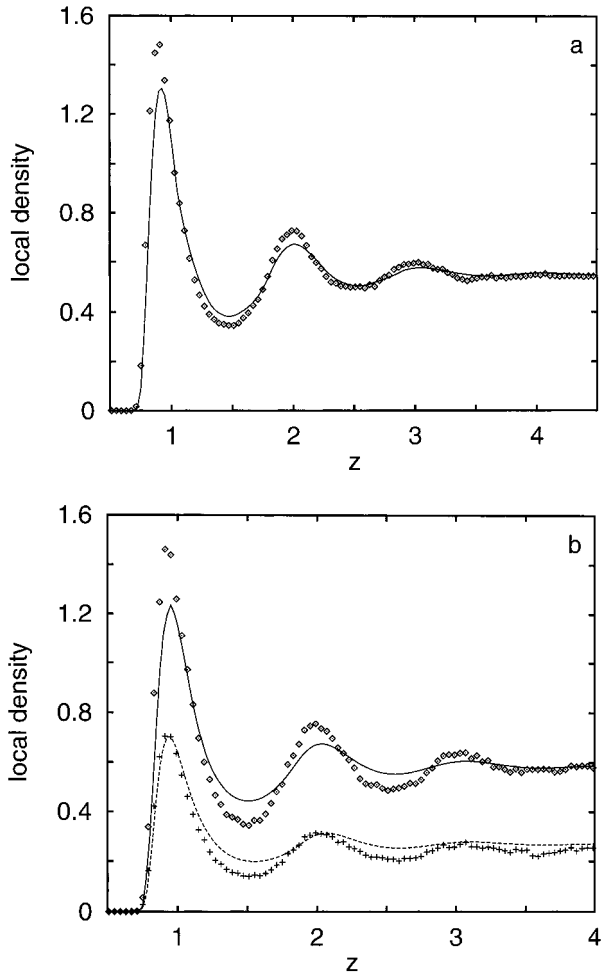

Figure 2. Same as in Figure 1, but for Lennard-Jones associating fluids: (a) $T^* = 2$, $\epsilon_a^* = 10$, and $\rho_b^* = 0.541$; (b) $T^* = 1.5$, $\epsilon_a^* = 15$, and $\rho_b^* = 0.578$.

of associating hard spheres is capable of reproducing correctly the fraction of unbounded particles.[11,12,28−30]

We know from the literature (cf. the review article of Evans[6]) that in the case of nonassociating hard spheres the weighted density functional theory works well for attractively adsorbing walls. It only begins to fail when the temperature is low and the bulk density takes on high values. In the case of the associating fluids investigated by us, the agreement with Monte Carlo data is less satisfactory. In particular, we observe that the oscillatory character of the DF density profiles is less pronounced than that found in simulations. The theory also underestimates the height of the first local density maximum. The profiles of bonded particles seem to be reproduced slightly better. The discrepancies are smaller if the energy of association is lower and if the system is less dense; cf. Figure 1a,b.

Parts a and b of Figure 2 compare the results for Lennard-Jones associating particles. Part a shows the results for very weak association; though the association energy is not too low, $\epsilon_a^* = \epsilon_a/\epsilon = 10$, the temperature is high, $T^* = kT/\epsilon = 2$, so at the bulk fluid density, $\epsilon_b^* = \rho_b\sigma^3 = 0.541$, the bulk ratio of unbounded particles is close to unity (simulation gives 0.986, whereas the theory estimates this ratio as equal to 0.989). For this reason we have plotted in Figure 2a only the density profile of all (dimerized and free) particles. Part b of Figure 2 is for $\epsilon_a^* = 15$, $T^* = 1.5$, and $\rho_b^* = 0.578$. The agreement of the simulated and theoretical results for LJ associating particles is slightly worse than in the case of associating hard spheres. Generally, the theory for associating Lennard-Jones fluid suffers from the same drawbacks as for associating hard spheres. A better agreement is found for lower association.

Taking into account the approximate character of the theory, we have not expected a nice agreement with simulations. The discrepancies can be attributed to the treatment of the associative contribution; cf. eq 15. One should keep in mind, however, that the bulk densities at which the comparisons with Monte Carlo data have been done are much higher than the densities at which usually experiments are carried out. Obviously, at lower densities the agreement should be much better. We now proceed to the second part of our work in which the DF theory is applied to study the wetting behavior of associating fluids near the wall.

3.2. Association in the Region of Prewetting Transition. The influence of association on the properties of bulk uniform systems has been a subject of numerous theoretical works.[28−31,36] It has been established that the increase in the association energy causes a gradual increase in the fluid critical temperature and leads to the widening of the coexistence region. Plots of such phase diagrams for several systems can be found in refs 28−30. On the other hand, effects of association in adsorption systems have attracted much less attention. To our best knowledge, the prewetting transition in associating systems has been studied[54] only via the constant pressure Monte Carlo method. The model used in ref 54 assumes, however, that the

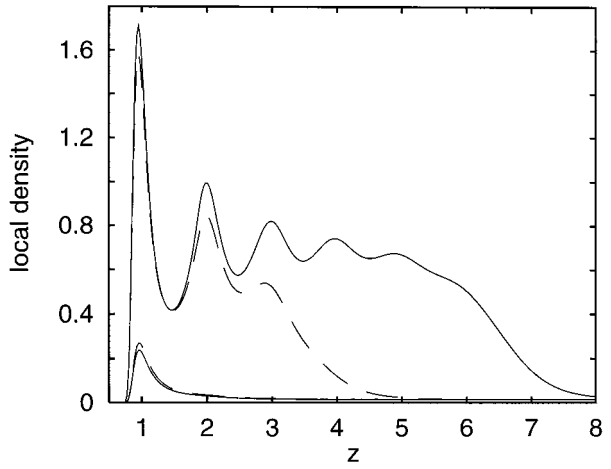

Figure 3. Density profiles for $\epsilon_a^* = 0.0$, $T^* = 0.9$. There are two pair of lines corresponding to thin and thick films. For each pair the lower curves are for $\rho_b^* = 0.014$ and the upper curves correspond to $\rho_b^* = 0.013$. The solid (dashed) lines are for the stable (metastable) states.

associating site is embedded into the core of a particle, which leads to dimers formed by overlapping spheres. A possibility of application of the density functional theory from refs 11−13 in such cases has been never tested; an alternative formulation of the density functional method proposed in ref 10 is much more computationally difficult to deal with. Thus, we have decided to consider the system of nonoverlapping particles, for which the density functional theory of Segura, Chapman, and co-workers[11,12] has been proved to give at least qualitatively correct results.

Since the prewetting transition may occur only for a weakly attractive surface,[55] we had to choose an appropriate value of the parameter ϵ_s. This value has been set as equal to 6.0. This corresponds to the relative strength of the fluid−fluid and the fluid−surface potential minima ≈2.31, which is close to the value characteristic for argon adsorbed on a solid carbon dioxide surface. The latter system has been intensively studied in several works.[14,17,23,24] To establish the effects of changes in the association energy on wettability of the model surface, we have considered three situations with $\epsilon_a^* = \epsilon_a/\epsilon = 0.0$, 7.0, and 10.0.

First we present the density profiles obtained for a simple nonassociative fluid, $\epsilon_a^* = 0$, at the temperature $T^* = kT/\epsilon = 0.9$, which is above the wetting temperature but well below the bulk critical point (the bulk critical temperature resulting from the bulk counterpart of the DF theory is $T_c^* = 1.305$). Figure 3 shows examples of the profiles at both sides of the prewetting van der Waals loop, obtained for two different values of the bulk density $\rho_b^* = 0.014$ and 0.013. The solid lines denote the stable states, which have been selected by analyzing the dependence of the grand potential Ω on the chemical potential. A stable state corresponds to the minimum of the grand potential. The dashed lines are the results representing metastable states. At the equilibrium between a thin and a thick film, the grand potential for two coexisting phases is identical. The bulk density corresponding to the coexistence point between the thin and thick film is $\rho_b^* = 0.0131$ at that temperature.

In Figure 4 we show the results obtained at the same temperature, but for associating systems with the association energy equal to 7. Part a of this figures displays the density profiles of all (dimerized and free) particles, while part b shows the fractions of nonassociated particles, χ, in the system. Only the profiles for thermodynamically stable states are shown here. The bulk density at which the prewetting transition occurs is $\rho_b^* = 0.009\,55$.

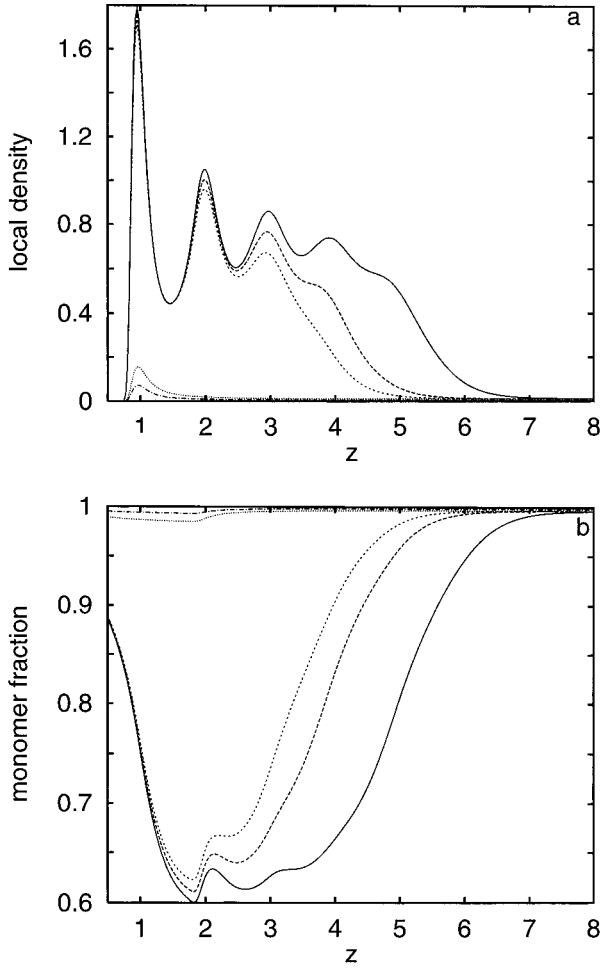

Figure 4. Density profiles (part a) and the fractions of nondimerized particles (part b) for the thermodynamically stable states at $T^* = 0.9$ and the association energy $\epsilon_a^* = 7.0$. The curves from top to bottom in part a, and from bottom to top in part b, correspond to $\rho_b^* = 0.010$, 0.0097, 0.0096, 0.0095, and 0.005.

We observe that the association leads to pronounced differences in the behavior of the system. In particular, we find that for the thick film the increase of the association energy causes an increase of the height of the first local density peak. On the contrary, the height of the local density maximum decreases in the region of small adsorption (below the prewetting transition). The density profiles of all (dimerized and free) particles corresponding to a thick film exhibit well-pronounced layered structure. However, the oscillations near the wall in the plot of the fraction of nondimerized particles (see part b of Figure 4) are significantly smaller. This is a direct consequence of the "local" mass action law: higher (lower) local concentration−higher (lower) local association. Consequently, the ratio of nondimerized particles remains nearly constant. For still higher association energy, $\epsilon_a^* = 10$, we have found that all the effects due to the association that have been found for $\epsilon_a^* = 7$ become more pronounced. To save space, the relevant figures have been omitted.

At a sufficiently small and high distance from the surface, the fraction of unbounded particles, $\chi(z)$, satisfies the boundary conditions

$$\lim_{z\to 0} \chi(z) = 1 \qquad \text{and} \qquad \lim_{z\to\infty} \chi(z) = \chi_b \tag{21}$$

where χ_b is the bulk (reference fluid) fraction of unbounded particles. Obviously, the increase of the association energy leads

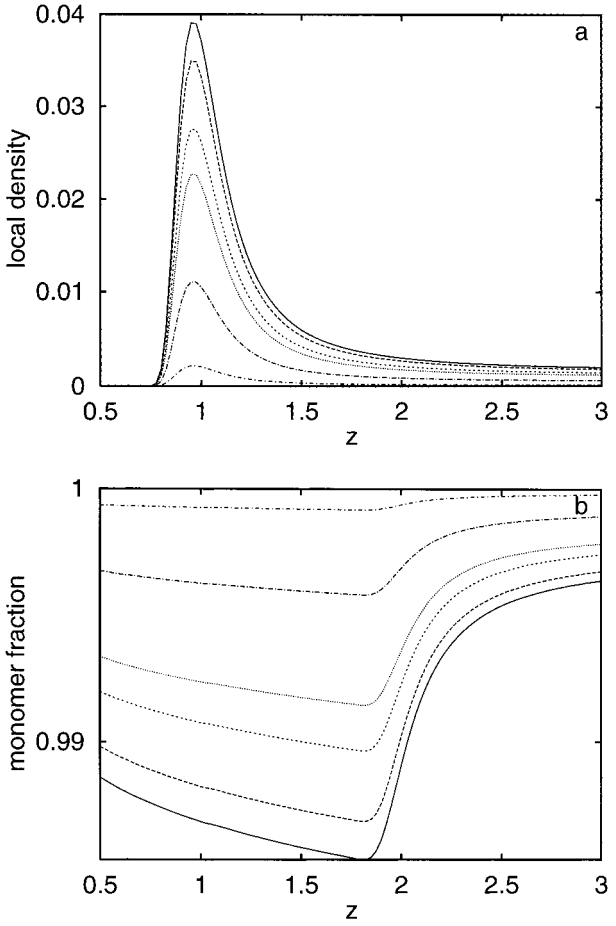

Figure 5. Density profiles (part a) and the fractions of nondimerized particles (part b) for $T^* = 0.7$ and the association energy $\epsilon_a^* = 7.0$. The curves from top to bottom in part a, and from bottom to top in part b, correspond to $\rho_b^* = 0.00162$, 0.0015, 0.0012, 0.001, 0.0005, and 0.0001.

to the decrease of the fraction of nondimerized particles in the film. We have compared the densities of nondimerized particles in a thick adsorbed film with the corresponding values for the bulk uniform liquid at the liquid densities at the coexistence line. For example, at $T^* = 0.9$ and for $\epsilon^* = 10$ the average profile density at its oscillating plateau (i.e., for $1.5 < z < 5$) is $\approx$0.786, whereas the bulk liquid density at the liquid−vapor coexistence point is $\approx$0.800. The fractions of undimerized particles at the plateau and in the bulk fluid at the equilibrium point are nearly the same and are equal to $\approx$0.16. In general, from our comparisons it appears that the average film density in the region of local density plateau (and except for the first adlayer) is slightly lower than the bulk coexistence density, whereas the fraction of undimerized particles is very close to its uniform liquid counterpart.

In order to demonstrate that the systems considered here exhibit nonzero wetting temperature, we have displayed the results of calculations for one system with $\epsilon_a^* = 7.0$ at the temperature equal to 0.7. Figure 5 shows evidently that only a thin (monolayer) film develops even at the bulk density extremely close to the bulk coexistence density, which equals to $\rho_b^*(T^* = 0.7) = 0.001\,654$. Part b of Figure 5 demonstrates that the surface effect on association is very low for thin film and both the film and the bulk gas consist mostly of nondimerized species. This contrasts sharply with the situation depicted in Figure 4b. Thus, the density of the film appears to be the most important factor determining the association extent at the surface.

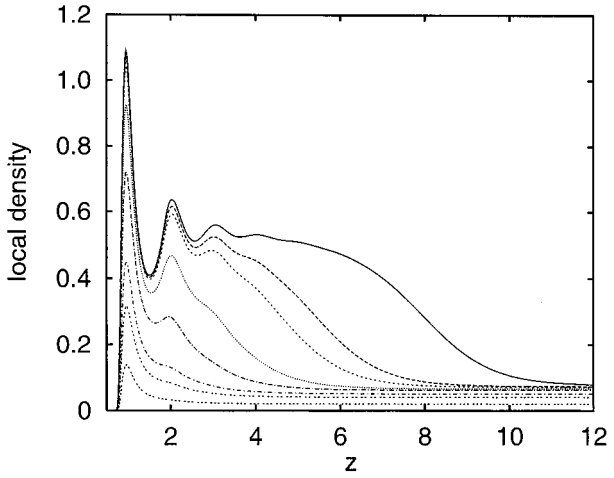

Figure 6. Density profiles for $T^* = 1.25$ and for the association energy $\epsilon_a^* = 10$. The curves from top to bottom correspond to $\rho_b^* = 0.075$, 0.072, 0.7, 0.065, 0.061, 0.055, 0.04, and 0.02.

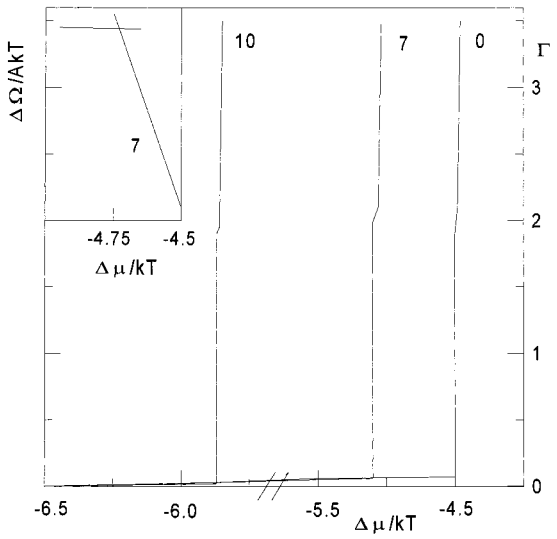

Figure 7. Examples of the adsorption at $T^* = 0.9$. The values of the association energy are given in the figure. The inset shows the plot of $\Delta\Omega$ vs the chemical potential. The intersection of two branches localizes the prewetting transition.

The first-order prewetting transition terminates at the surface critical temperature; above that temperature the thick film development is continuous. This point is illustrated in Figure 6, where we have displayed the density profiles for the system with $\epsilon_a^* = 10$ and at $T^* = 1.25$. No double solutions of the density profile equation have been found in this case and the adsorbed film grows continuously.

The density profiles have been integrated to evaluate the adsorption isotherms Γ,

$$\Gamma = \int_0^\infty [\rho(z) - \rho_b]\, dz \qquad (22)$$

Examples of results emerging from such calculations, carried out at $T^* = 0.9$ are shown in Figure 7. All adsorption isotherms displayed here exhibit a prewetting jump. At sufficiently low bulk densities only thin films at the surface occur. As the density equals the wetting density, a discontinuity step on the isotherm develops. The inset illustrates how this step was localized. Namely, the locus of the transition has been found from the plot of $\Delta\Omega = \Omega - \Omega_b$, where Ω_b is the grand canonical potential for a bulk uniform fluid of density ρ_b, versus the

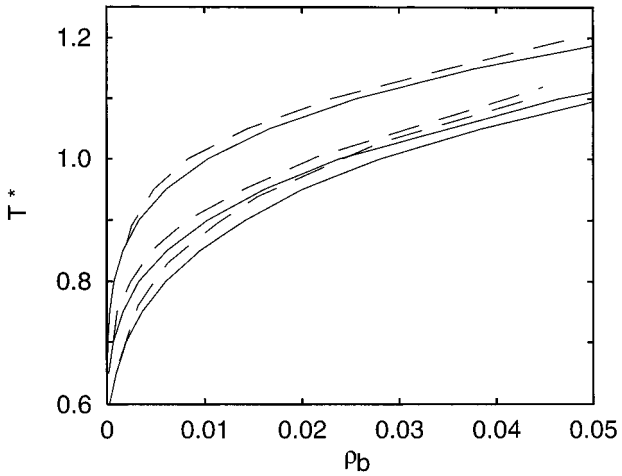

Figure 8. Phase diagrams for nonassociating and associating systems. The solid lines denote the bulk coexistence while the dashed lines denote the location of the prewetting transition.

TABLE 1: Bulk Critical Temperatures, T_c^*, Wetting Temperatures, T_w^*, and the Surface Critical Temperatures, T_{sc}^*, Resulting from the Density Functional Theory for the Systems Considered in This Work

ϵ_a^*	T_c^*	T_w^*	T_{sc}^*
0	1.305	0.68	1.09
7	1.335	0.72	1.12
10	1.385	0.85	1.19

chemical potential. The prewetting transition occurs at the chemical potential at the intersection of two branches corresponding to a thin and thick film. The value of ρ_b is next estimated from the bulk counterpart of the theory. When the association energy increases, the prewetting jump shifts toward lower bulk densities.

Similar calculations have been performed at several temperatures. In particular for each association energy we find the surface critical temperature at and above which the wetting becomes continuous and the wetting temperature at and below which the isotherm remains finite (Langmuirian-like) up to the bulk coexistence density. The observed behavior is the same as for simple fluids.[6] However, the main effect of association is the shift of the wetting and the surface critical temperatures toward higher values.

The summary of our computations is presented in Figure 8. There are lines showing the locations of the prewetting transition, each of them begins at the wetting temperature, T_w^*, and terminates at the surface critical temperature, T_{sc}^*, above which the wetting transition is continuous. The values of T_w^* and T_{sc}^* are collected in Table 1. We find that both T_w^* and T_{sc}^* increase with the association energy. In particular, our estimation of the wetting temperature is $T_w^* = 0.68$ for a nonassociating system and $T_w^* = 0.85$ for $\epsilon_a^* = 10$. Now, let us compare our results obtained for the nonassociative system with those reported previously. We have already noted that for $\epsilon_a^* = 0$ the system under study is close to the model of argon adsorbed on solid carbon dioxide. The latter system has been studied in several works.[14,17,23,24,46,47,56−59] The Monte Carlo simulations of Finn and Monson[23] led to T_w^*, $= 0.84 \pm 0.01$ and $T_{sc}^* = 0.94 \pm 0.02$. It should be noted, however, that they have assumed the cutoff distance of the Lennard-Jones potential (2) equal to $r_{cut} = 2.5\sigma$. On the other hand, the molecular dynamics studies carried out without any cutoff distance estimated that $T_w^* \in [0.95, 1]$.[24] This may be compared with the DF theory of Meister and Kroll that gave $T_w^* = 1.25$.[17]

Comparing our results with the literature data, one should remember that the WCA division of the interparticle potential (2) is not unique. In fact, different methods of division of the Lennard-Jones potential into repulsive and attractive parts have been considered (cf. ref 6). In particular, some modifications to $u_{att}(r)$ have been sometimes made[6,57] to ensure a better bulk equation of state. Obviously, both characteristic temperatures T_{sc}^* and T_w^* depend on the details of the potential model. For example, Valesco and Tarazona[57] have introduced an adjustable parameter into their definition of the attractive branch of the Lennard-Jones potential to ensure that the bulk coexistence curve obtained from the bulk counterpart of the density functional theory is identical to that obtained from simulation. The theoretical result for the surface critical temperature of Valecso and Tarazona is $T_{sc}^* = 0.96 \pm 0.01$, while the wetting temperature has been found to be lower than 0.74. The latter estimation is close to our result.

4. Conclusions

Let us now conclude our results. In this paper we have presented the application of the density functional theory to study the wetting behavior of nonuniform associating fluids in contact with attractive walls. The most interesting finding is the demonstration of changes in the behavior of the fluid−wall interface resulting from the dimerization of fluid particles. In particular, it has been shown that association shifts the wetting temperature as well as the surface critical temperature, associated with the prewetting transition, toward higher values. From the data given in Table 1 it follows that the effect of association on T_{sc}^* is very similar to that observed for the bulk critical temperature. On the other hand, the changes in the wetting temperature, caused by an increasing tendency to association, are considerably greater. In order to explain the above findings, we first note that monomers and dimerized species form a binary mixture. The interaction between a pair of dimers is stronger than between a pair of monomers (as well as between a mixed, monomer−dimer, pair). The magnitude of critical temperature, either bulk or surface, is proportional to the average pair interaction energy. Thus, the increasing tendency toward formation of dimers leads to the increase of the average interparticle interaction energy. The same effect is responsible for the observed increase of the wetting temperature with the increase of association energy. In general, the wetting behavior at the fluid−solid interface is determined by the relative strength of the fluid−fluid and the fluid−solid interactions. When the fluid−fluid interaction energy increases with respect to the fluid−solid interaction energy, the wetting temperature also increases. In the situation considered here, the energy of interaction between the adsorbed dimer and the wall is stronger than between the adsorbed monomer and the wall, and one might expect that a sort of compensation effect appears, leaving the wetting temperature more or less unchanged. This is not the case here, since the difference between the monomer−wall and the dimer−wall interaction energy is smaller than the difference between the energies of fluid−fluid interactions in the simple (monomeric) fluid and in the highly dimerized fluid. To a first approximation we can say that the interaction of fully dimerized fluid with the wall is about 2 times greater than the interaction between the monomer and the wall. On the other hand, the interaction between just a single pair of dimers is more than 2 times stronger than the monomer−monomer interaction. Therefore, the effective ratio of the fluid−fluid and the fluid−wall interactions

increases when the association extent grows. Besides, we have found that the concentration of dimerized species is highly anisotropic, and such particles prefer to stay near the wall. This explains why the dimerization more strongly influences the wetting temperature than the surface critical temperature, which depends on the dimer concentration in the entire film.

The above explanation can be readily checked by assuming different interaction parameters for bonded and unbounded particles or by considering models with different bond lengths. We plan to report on those problems in a future work.

Acknowledgment. We are grateful to O. Pizio (UNAM) for helpful discussions. This work was supported by the KBN under the Grant No 3 T09A 062 10.

References and Notes

(1) Jamnik, A.; Bratko, D. *Chem. Phys. Lett.* **1993**, *203*, 465.
(2) Holovko, M. F.; Vakarin, E.V. *Mol. Phys.* **1995**, *84*, 1057.
(3) Holovko, M. F.; Vakarin, E. V. *Mol. Phys.* **1996**, *87*, 1375.
(4) Henderson, D.; Sokołowski, S.; Pizio, O. *J. Chem. Phys.* **1995**, *102*, 9048.
(5) Henderson, D.; Sokołowski, S.; Trokhymchuk, A. J. *Chem. Phys.* **1995**, *103*, 4693.
(6) Evans, R. In *Fundamentals of Inhomogeneous Fluids*; Henderson, D., Ed.; Marcel Dekker: New York, 1992.
(7) Kierlik, E.; Rosinberg, M. L. *J. Chem. Phys.* **1992**, *97*, 9222.
(8) Kierlik, E.; Rosinberg, M. L. *J. Chem. Phys.* **1993**, *99*, 3950.
(9) Kierlik, E.; Rosinberg, M. L. *J. Chem. Phys.* **1994**, *100*, 1716.
(10) Trokhymchuk, A.; Henderson, D.; Sokołowski, S. *Phys. Lett. A* **1995**, *245*, 615.
(11) Segura, C. J.; Chapman, W.; Shukla, K. P. *Mol. Phys.* **1997**, *90*, 759.
(12) Segura, C. J.; Vakarin, E. V.; Chapman, W. G.; Holovko, M. F. *J. Chem. Phys.* **1998**, *108*, 4837.
(13) Henderson, D.; Patrykiejew, A.; Sokołowski, S. *Mol. Phys.* **1998**, *95*, 211.
(14) Ebner, C.; Saam, W. F. *Phys. Rev. Lett.* **1977**, *38*, 1486.
(15) Tarazona, P. *Phys. Rev. A* **1985**, *31*, 2672.
(16) Bruno, E.; Cacamo, C.; Tarazona, P. *Phys. Rev. A* **1987**, *35*, 1210.
(17) Meister, T. F.; Kroll, D. M. *Phys. Rev. A* **1985**, *31*, 4055.
(18) Chmiel, G.; Patrykiejew, A.; Rżysko, W.; Sokołowski, S. *Mol. Phys.* **1994**, *83*, 19.
(19) Henderson, D.; Patrykiejew, A.; Sokołowski, S. *Mol. Phys.* **1995**, *85*, 745.
(20) Forgacs, G.; Lipowsky, R.; Nieuwenhuizen, Th. M. In *Phase Transitions and Critical Phenomena*; Domb, C., Lebowitz, J. L., Eds.; Academic Press: London, 1991; Vol. 14.
(21) Chmiel, G.; Patrykiejew, A.; Rzysko, W.; Sokołowski, S. *Phys. Rev. B* **1993**, *48*, 14454.
(22) Binder, K. Thin Films and Phase Transitions at Surfaces. In *Proceedings of the East-West-Surface Science Workshop EWSSW 94*, 14−20 Feb 1994; Pamparowo: Sophia, Bulgaria; 1994.
(23) Finn, J. E.; Monson, P. A. *Phys. Rev. A* **1989**, *39*, 6402.
(24) Sokołowski, S.; Fischer, J. *Phys. Rev. A* **1990**, *41*, 6866.
(25) van Swol, F.; Henderson, J. R. *J. Chem. Soc., Faraday Trans 2* **1986**, *82*, 1685.
(26) Sikkenk, J. H.; Indeku, J. O.; van Leeuwen, J. M. J.; Vosnack, E. O. *Phys. Rev. Lett.* **1987**, *59*, 98.
(27) Wertheim, M. S. *J. Chem. Phys.* **1987**, *87*, 7323.
(28) Jackson, G.; Chapman, W. G.; Gubbins, K. *Mol. Phys.* **1988**, *65*, 1.
(29) Johnson, K.; Gubbins, K. *Mol. Phys.* **1992**, *77*, 1033.
(30) Joslin, C. G.; Gray, C. G.; Chapman, W. G.; Gubbins, K. *Mol. Phys.* **1987**, *62*, 843.
(31) Sokołowski, S.; Trokhymchuk, A. *Phys. Lett. A* **1997**, *236*, 557.
(32) Haymett, A. D. J. In *Fundamentals of Inhomogeneous Fluids*; Henderson, D., Ed.; Marcel Dekker: New York, 1992.
(33) Curtin, W. A; Ashcroft, N. W. *Phys. Rev. A* **1985**, *32*, 2909.
(34) Denton, A. R.; Ashcroft, N. W. *Phys. Rev. A* **1989**, *39*, 426, 4701.
(35) Calleja, M.; Rickayzen, G. *Mol. Phys.* **1989**, 791−993.
(36) Rocken, P.; Somoza, A.; Tarazona, P.; Findenegg, G. *J. Chem. Phys.* **1998**, *108*, 8689.
(37) Golzelman, B.; Dietrich, S. *Phys. Rev. E* **1997**, *55*, 2993.
(38) Groot, R. D. *Mol. Phys.* **1989**, *60*, 45.
(39) Sokołowski, S.; Fischer, J. *Mol. Phys.* **1989**, *68*, 647.
(40) Rosenfeld, Y. *Phys. Rev. Lett.* **1989**, *63*, 980.
(41) Kierlik, E.; Rosinberg, M. L. *Phys. Rev. A* **1990**, *42*, 3383.
(42) Kierlik, E.; Fan, Y.; Monson, P. A.; Rosinberg, M. L. *J. Chem. Phys.* **1995**, *102*, 3712.
(43) Tarazona, P.; Rosenfeld, Y. *Phys. Rev. E* **1997**, *55*, R4873.
(44) Curtin, W. A.; Ashcroft, N. W. *Phys. Rev. Lett.* **1986**, *56*, 2775.
(45) Powles, J. G.; Rickayzen, G.; Williams, M. L. *Mol. Phys.* **1988**, *64*, 33.
(46) Tang, Z.; Scrivien, L. E.; Davis, H. T. *J. Chem. Phys.* **1991**, *95*, 2659.
(47) Sokołowski, S.; Fischer, J. *J. Chem. Phys.* **1992**, *96*, 5441.
(48) Weeks, J. D.; Chandler, D.; Andersen, H. C. *J. Chem. Phys.* **1971**, *54*, 5237.
(49) Tarazona, P.; Marconi, U. M. B.; Evans, R. *Mol. Phys.* **1987**, *60*, 573.
(50) Carnahan, N. F.; Starling, K. E. *J. Chem. Phys.* **1969**, *51*, 635.
(51) Chapman, W. G. *J. Chem. Phys.* **1990**, *93*, 4299.
(52) Duda, Y.; Pizio, O.; Sokołowski, S. *Czech. J. Phys.*, in press.
(53) Duda, Y.; Pizio, O.; Sokołowski, S.; Trokchymchuk, A. *J. Colloid Interface Sci.* **1997**, *194*, 68.
(54) Borówko, M.; Patrykiejew, A.; Sokołowski, S.; Zagerski, R. *J. Chem. Soc., Faraday Trans. 1* **1998**, *94*, 771.
(55) Pandit, R.; Schick, M.; Wortis, M. *Phys. Rev. B* **1982**, *26*, 5112.
(56) Evans, R.; Tarazona, P. *Mol. Phys.* **1984**, *52*, 847.
(57) Valesco, E.; Tarazona, P. *Phys. Rev. A* **1990**, *42*, 2454.
(58) Davis, H. T. *J. Chem. Phys.* **1984**, *80*, 589.
(59) Teletzke, C.; Scrivien, L. E.; Davis, H. T. *J. Colloid Interface Sci.* **1982**, *87*, 550.